

PLEIAD/SIMC1/C5orf25, a Novel Autolysis Regulator for a Skeletal-Muscle-Specific Calpain, CAPN3, Scaffolds a CAPN3 Substrate, CTBP1

Yasuko Ono^{1,2}, Shun-ichiro Iemura^{1,3}, Stefanie M. Novak², Naoko Doi¹, Fujiko Kitamura¹, Tohru Natsume³, Carol C. Gregorio² and Hiroyuki Sorimachi¹

1 - Calpain Project, Department of Advanced Science for Biomolecules, Tokyo Metropolitan Institute of Medical Science (IGAKUKEN), 2-1-6 Kamikitazawa, Setagaya-ku, Tokyo 156-8506, Japan

2 - Cellular and Molecular Medicine, University of Arizona, Tucson, AZ 85724, USA

3 - Biological Information Research Center, National Institute of Advanced Industrial Science and Technology, 2-42 Aomi, Kohtoh-ku, Tokyo 135-0064, Japan

Correspondence to Yasuko Ono: Calpain Project, Department of Advanced Science for Biomolecules, Tokyo Metropolitan Institute of Medical Science, 2-1-6 Kamikitazawa, Setagaya-ku, Tokyo 156-8506, Japan. ono-ys@igakuken.or.jp
<http://dx.doi.org/10.1016/j.jmb.2013.05.009>

Edited by R. Huber

Abstract

CAPN3/p94/calpain-3 is a skeletal-muscle-specific member of the calpain protease family. Multiple muscle cell functions have been reported for CAPN3, and mutations in this protease cause limb-girdle muscular dystrophy type 2A. Little is known about the molecular mechanisms that allow CAPN3 to be so multifunctional. One hypothesis is that the very rapid and exhaustive autolytic activity of CAPN3 needs to be suppressed by dynamic molecular interactions for specific periods of time. The previously identified interaction between CAPN3 and connectin/titin, a giant molecule in muscle sarcomeres, supports this assumption; however, the regulatory mechanisms of non-sarcomere-associated CAPN3 are unknown. Here, we report that a novel CAPN3-binding protein, PLEIAD [*Platform element for inhibition of autolytic degradation*; originally called SIMC1/C5orf25 (SUMO-interacting motif containing protein 1/chromosome 5 open reading frame 25)], suppresses the protease activity of CAPN3. Database analyses showed that PLEIAD homologs, like CAPN3 homologs, are evolutionarily conserved in vertebrates. Furthermore, we found that PLEIAD also interacts with CTBP1 (*C-terminal binding protein 1*), a transcriptional co-regulator, and CTBP1 is proteolyzed in COS7 cells expressing CAPN3. The identified cleavage sites in CTBP1 suggested that it undergoes functional modification upon its proteolysis by CAPN3, as well as by conventional calpains. These results indicate that PLEIAD can shift its major function from CAPN3 suppression to CAPN3-substrate recruitment, depending on the cellular context. Taken together, our data suggest that PLEIAD is a novel regulatory scaffold for CAPN3, as reflected in its name.

© 2013 The Authors. Published by Elsevier Ltd. Open access under [CC BY license](http://creativecommons.org/licenses/by/3.0/).

Introduction

CAPN3 (also called p94 or calpain-3) is an skm (*skeletal muscle*)-specific cysteine protease belonging to the calpain super family (EC 3.4.22.18, clan CA, family C2).¹ The calpains are intracellular Ca²⁺-requiring cysteine proteases. Many studies have shown that proteolysis by calpain has a modulatory effect on the functions of the substrate proteins.²⁻⁶ Therefore, calpain is considered to be a modulator

protease rather than a degrading protease such as proteasomal and lysosomal proteases.⁷

From a physiological perspective, genetic defects in CAPN3 cause limb-girdle muscular dystrophy type 2A⁸; therefore, the importance of CAPN3's functions are well recognized.⁹ To examine the consequences of altering the modulating functions of CAPN3 in skm, we have generated several different mouse limb-girdle muscular dystrophy type 2A models, including knockout mice (*Capn3*^{-/-}), which lack the full-length CAPN3 protein¹⁰⁻¹⁷; knockin mice (*Capn3*^{CS/CS}) in

which CAPN3 is replaced by a protease-inactive mutant CAPN3:C129S (CAPN3:CS)^{18,19}; and transgenic mice in which CAPN3:CS is overexpressed.²⁰ Analyses of these models have shown that CAPN3 has different cellular functions depending on the subcellular compartment in which it is located. In particular, a surprising finding was that CAPN3 localizes to triads, where it plays an important role as a structural component and not as a protease.¹⁹

The two defined roles of CAPN3, that is, as a protease and as a structural protein, are not necessarily mutually exclusive. However, too little is currently known about the molecular properties of CAPN3 to explain the relationships among these two roles and another property of CAPN3—its very rapid autolysis.²¹ In skm cells, CAPN3's stability as a pre-autolytic full-length molecule has been attributed to its interaction with connectin/titin, a giant sarcomeric protein,^{22,23} since connectin/titin's ability to suppress the autolytic loss of CAPN3 has been shown biochemically.²⁴ Furthermore, the N2A region of connectin/titin has been suggested to function as a scaffold for CAPN3.^{25,26} However, in skm cells, CAPN3 is stable not only in sarcomeres but also in the cytosol.²⁷ Therefore, it is predicted that there are other regulatory mechanisms working in parallel or in combination with the connectin/titin-based machinery, to support CAPN3's multiple functions, especially those occurring outside of sarcomeres.

We sought to identify CAPN3-interacting proteins using a highly sensitive and efficient method based on mass spectrometry for analyzing protein–protein interactions.²⁸ Among these proteins, PLEIAD (*P*latform element for *i*nhibition of autolytic *d*egradation), which was the previously uncharacterized SIMC1/C5orf25 (SUMO-interacting motif containing protein 1/ chromosome 5 open reading frame 25),²⁹ demon-

strated a suppressive effect on CAPN3's protease activity. We identified vertebrate orthologs of PLEIAD according to their similarity with the human C-terminal sequence, which harbors the CAPN3 inhibitory or regulatory activity. We also found that PLEIAD binds to CTBP1 (*C*-terminal binding protein 1),^{30,31} which is a good substrate for calpains, including CAPN3. These results suggest that SIMC1/C5orf25 is a suppressor for CAPN3 but, at the same time, scaffolds CAPN3 to direct and regulate its substrate-proteolyzing activity. Such properties, like those of the connectin/titin N2A region, would qualify PLEIAD as an important regulatory protein for CAPN3.

Results

Protease activity of CAPN3 is suppressed by a novel protein, PLEIAD

To explore molecular interactions relevant to CAPN3's function and regulation, we expressed FLAG-CAPN3:N358D (CAPN3:ND), an activity-attenuated mutant³² (Fig. 1a), in HEK293 cells and analyzed anti-FLAG coimmunoprecipitates of HEK293 lysates by liquid chromatography coupled with tandem mass spectrometry.²⁸ Since the initial goal was to identify activation-dependent interactions, the cells were treated with the Ca²⁺-ionophore A23187, and the results were compared to those obtained in cells without A23187 treatment. This approach identified a novel CAPN3-binding protein C5orf25, which we named PLEIAD (see below) (Fig. 1b). To confirm the interaction, we expressed both proteins in COS7 cells; the interaction between MYC-PLEIAD and FLAG-CAPN3, as well as the interaction between FLAG-PLEIAD and CAPN3,

Fig. 1. A novel human protein, PLEIAD/C5orf25, interacts with and suppresses CAPN3. (a) Structure of CAPN3 is schematically shown. Autolytic activity is based on the result when each construct is expressed in COS7 cells. Vertical arrows indicate predominant autolytic sites. PC1 and PC2, protease core domains 1 and 2; C2L, C2-domain-like; PEF (L), penta-EF-hand; NS/IS1/IS2, CAPN3-specific insertion sequences; C129/H334/N358, active-site amino acid residues Cys, His, and Asn; CAPN3:CS, protease-inactive mutant; CAPN3:ND, a mutant with attenuated protease activity. (b) Domain structure of hPLEIAD and its genomic structure. Transcript variants are also depicted. The sequence information is summarized in Table 2. hPLEIADa to e, known splicing variants. hPLEIADf, the novel splicing variant of PLEIAD identified in this study, which lacks exons 2 and 3. "S1" to "S3" and "AS1" to "AS4" represent the positions of sense and antisense primers, respectively, used in the study. The sequences are summarized in Table 1. Ser and Pro, Ser-rich and Pro-rich region, respectively; PEST, a region rich in Pro, Glu, Ser, and Thr; NLS, putative nuclear localization signal sequence. Two phosphorylation sites are identified in hPLEIAD, S651 and S791. (c) hPLEIADf was coexpressed with CAPN3:WT(WT) or CAPN3:CS(CS) in COS7 cells and immunoprecipitated by anti-FLAG (FLAG-IP). Both CAPN3:WT and CAPN3:CS were coimmunoprecipitated with hPLEIADf. Note that the full-length 94-kDa band was hardly detectable when CAPN3:WT was expressed alone (lane 1, anti-pIS2). In the presence of coexpressed hPLEIADf, the 94-kDa band became visible and appeared to be coimmunoprecipitated more efficiently than the 55-kDa autolyzed fragment (lanes 4 and 9). (d) When coexpressed with PLEIADa or hPLEIADf in COS7 cells, the intensity of the full-length 94-kDa band of CAPN3:WT relative to that of the 55-kDa autolyzed fragment increased (lanes 4 and 5, anti-CAPN3). In the same samples, generation of the proteolyzed fragment of fodrin was suppressed (lanes 4 and 5, anti-proteolyzed fodrin). When the amount of the expression plasmid for hPLEIADf was reduced, the effects were smaller, and a decrease in expressed hPLEIADf was observed (lane 6). Closed and open arrowheads indicate the full-length and autolytic fragments of CAPN3, respectively, detected by Western blotting using an anti-pIS2 antibody. (e) Signal intensity of the full-length 94-kDa band evaluated using the intensity of the autolytic 55-kDa band in the same lane as a standard (e).

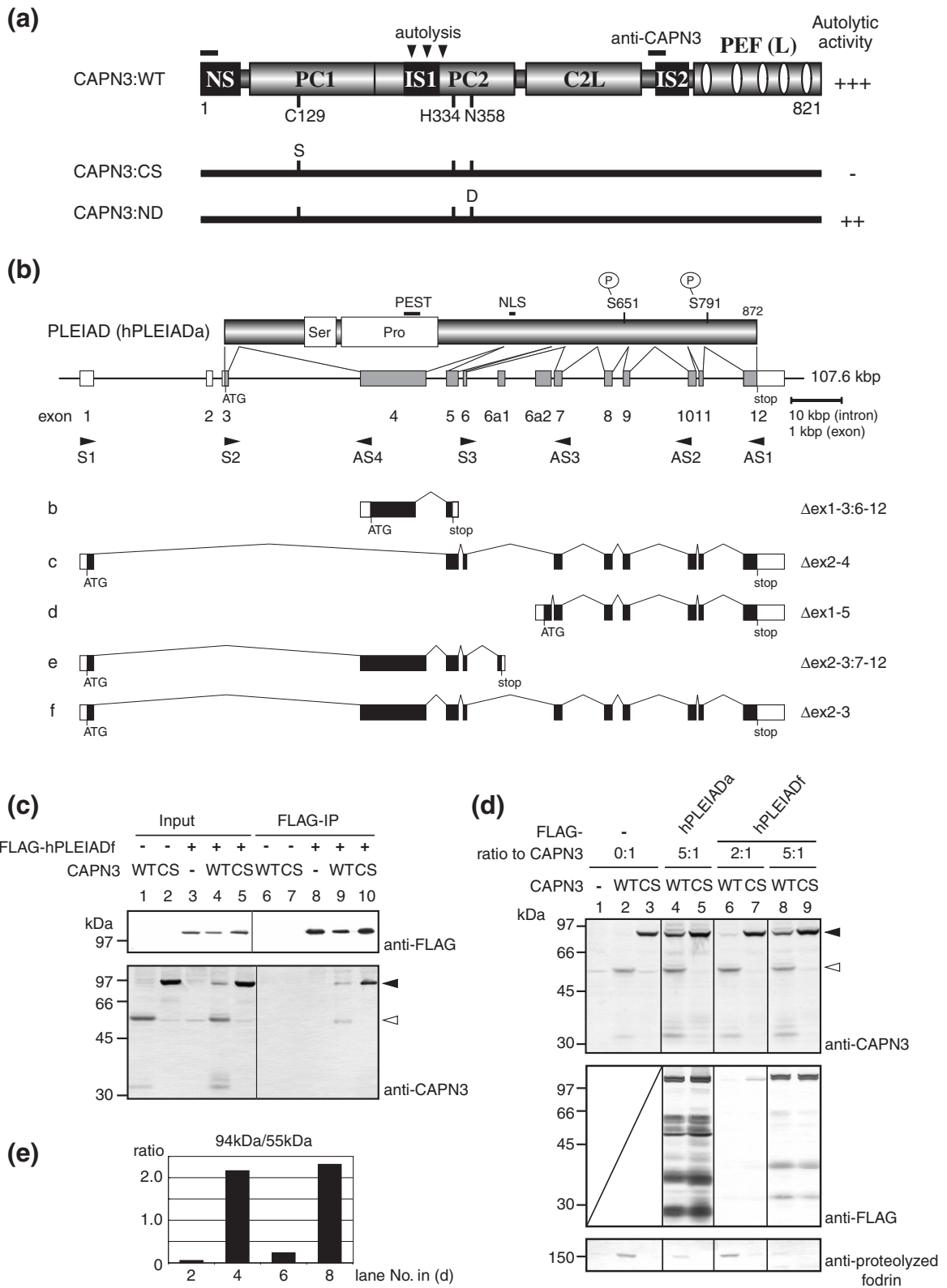


Fig. 1 (legend on previous page)

was reproducible without A23187 treatment (data not shown). Therefore, A23187 was omitted in the subsequent experiments.

The human PLEIAD gene (*PLEIAD*) is composed of 12 exons, of which exon 3 encodes the canonical first Met (Fig. 1b). In the National Center for Biotechnology Information (NCBI) and UniProtKB databases, the sequences for several alternative transcripts and corresponding proteins are deposited.³³ None of them, however, contains the sequence corresponding to exons 2 and 3. By PCR using a human skm cDNA library, we identified a novel variant lacking exons 2 and 3, but none of the other variants was found in the database [Fig. 1b, (5)]. This isoform will be temporarily designated as hPLEIADf.

Anti-FLAG coimmunoprecipitation experiments demonstrated the interaction of FLAG-hPLEIADf with CAPN3:WT and CAPN3:CS (Fig. 1c, lanes 9 and 10, anti-CAPN3). Therefore, the interaction between PLEIAD and CAPN3, which was originally detected in HEK293 cells, is predicted to take place in skm cells. Notably, the amount of FLAG-hPLEIADf was decreased when coexpressed with CAPN3:WT (compare lanes 4 and 5, anti-FLAG), and the relative intensity of the full-length 94-kDa band of CAPN3:WT was increased in the same sample (compare lanes 1 and 4, anti-CAPN3). This phenomenon is likely to indicate that CAPN3 activity reduces the amount of PLEIAD, either directly by proteolyzing it or indirectly by reducing the efficiency of PLEIAD's expression, and that PLEIAD reduces the autolytic activity of CAPN3.

These trends were confirmed by several independent transfections, and one representative result is shown in Fig. 1d. The signal intensity of the full-length 94-kDa band was evaluated using the intensity of the autolytic 55-kDa band in the same lane as a standard (Fig. 1e). Both hPLEIADa and hPLEIADf increased the amount of the 94-kDa

CAPN3:WT, which was dependent on the level of hPLEIADf (lanes 4, 6, and 8, anti-CAPN3). Since the CAPN3-dependent proteolysis of fodrin was also suppressed (lanes 4 and 8 compared with lane 2, anti-proteolyzed fodrin), it was concluded that the protease activity of CAPN3 is suppressed by PLEIAD. Multiple bands were observed for hPLEIADa and hPLEIADf (Fig. 1d, lanes 4, 5, 8, and 9), independent of CAPN3's protease activity. Since FLAG tags were introduced to the N-termini of the hPLEIADs, the observed molecular sizes of these bands suggested that the region encoded by exon 4 is susceptible to nonspecific proteolysis in the cell.

The C-terminal region of PLEIAD regulates CAPN3's autolysis

To define the functional domains of PLEIAD with respect to their effect on CAPN3 autolysis, we coexpressed two different PLEIAD regions with CAPN3 in COS7 cells.

When the C-terminal region, designated as hPLEIAD-C, was coexpressed with CAPN3, the amount of CAPN3 detected by anti-CAPN3 increased. That is, the relative intensity of the 94-kDa band of CAPN3:WT increased, indicating reduced autolytic activity, but not as much as with the coexpression of hPLEIADa or hPLEIADf (Fig. 2b, lane 3 *versus* Fig. 1d, lanes 4 and 8, anti-CAPN3). In contrast, the N-terminal region of hPLEIAD, called hPLEIAD-N, had no effect on the expression pattern or intensity of CAPN3 (lane 4). These findings suggested that the conserved C-terminal sequence retained the CAPN3-suppressing activity, although it was weaker than the suppression exerted by full-length hPLEIADa and hPLEIADf.

For the mouse PLEIAD ortholog (mPLEIAD, originally called LOC319719), the structure of its gene, *Pleiad* (originally called *4732471D19Rik*), is similar to that of human *PLEIAD* (Fig. 2c). There are,

Fig. 2. The C-terminal region of PLEIAD is responsible for regulating CAPN3's autolytic activity. (a) Two regions of PLEIAD, hPLEIAD-N [corresponding to exons 1–4, lacking the sequence from 368 aa to 458 aa (91 aa) and having an additional sequence, LDICCS, in its C-terminus] and hPLEIAD-C (exons 5–12) were coexpressed with CAPN3:WT or CAPN3:CS in COS7 cells. PLEIAD homologs identified by psi-BLAST search share homology with the sequence of hPLEIAD-C (Tables 2 and 3). (b) When the C-terminal region, hPLEIAD-C, was coexpressed, the 94-kDa band of CAPN3:WT was visible (lane 3). However, the effect was not as dramatic as that observed with full-length PLEIAD (Fig. 1d, lanes 4 and 8). Notably, in the same sample, the intensity of the bands for autolyzed fragments was increased. The same patterns were observed for cells in which CAPN3:CS was coexpressed with either fragment of PLEIAD (lanes 6 and 7). Closed and open arrowheads indicate the full-length and autolytic fragments of CAPN3, respectively, detected by Western blotting using an anti-pS2 antibody. (c) Mouse PLEIAD, mPLEIAD/LOC319719, is encoded by *Pleiad* (originally called *4732471D19Rik*). In this gene, the exons corresponding to exons 2 and 3 in the human *PLEIAD* are not defined. The largest gene product (mPLEIADa) is composed of 1354 aa, which is much larger than any isoforms of hPLEIAD. The structure of mPLEIADb is essentially identical with that of hPLEIADc. S3 and AS2 indicate the position of primers used in (d). The primer sequences are summarized in Table 1. (d) Expression of *Pleiad* detected by RT-PCR. In myotubes, a splicing variant of CAPN3 without exons 15 and 16 was also faintly detected (lane 11, lower band). W, H₂O was used as a template; – and +, isolated total RNA before and after, respectively, the RT reaction, was used as template; M, size marker. Qc, quadriceps from a 30-week-old mouse; Mt5, myotubes developed for 5 days from a primary culture of mouse myoblasts. Expected product sizes for *Capn3* (by primers CAPN3_411 and 412) and *Pleiad* (S3 and AS2) were 547 bp and 492 bp, respectively.

however, two markedly different features: the exons corresponding to human exons 2 and 3 are not identifiable, and exon 2, which by definition corre-

sponds to human exon 4, is expanded (Fig. 2c). Reverse transcription (RT)-PCR analysis using primers S3 and AS2 (Fig. 2c) revealed that

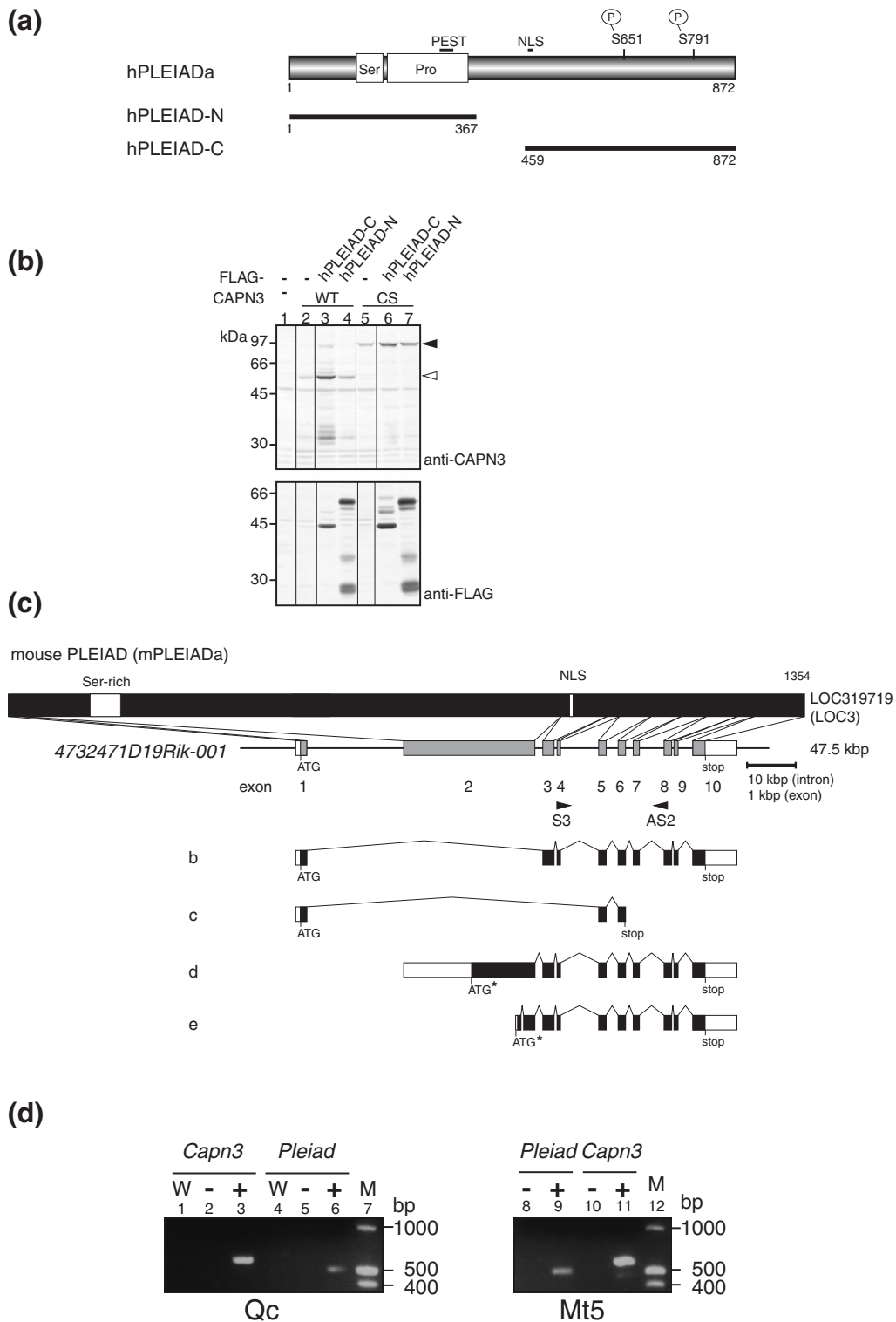


Fig. 2 (legend on previous page)

Table 1. Primers used in this study for cDNA cloning and RT-PCR detection

Primer	Reference sequence no.	Position ^a	Sequence
S1	BC037298	143–159s	cggtcggtaCCCGyAGCCATGGAGGA ^b
S2		417–439s	aacacatATGGCACCAGCATCTGCTTCTGG ^b
S3 ^c		2071–2090s	TCACCTATGTCATGGAGGAA
AS1		3065–3048as	GGAGAGAGAGTTCAGGAGG
AS2 ^c		2545–2562as	GGTGGCTTTCCATGGTAG
AS3		2155–2170as	AGGGTCTGCTGAAAGT
AS4		739–759as	GGTCCAAATCTACAGGATCAC
CAPN3_411	NM_000070.2	1801–1820s	CTCTT CACCA TTGGC TTCGC,
CAPN3_412		2347–2367as	CAGGTCCTTGTGTTTGTTCAC

^a s, sense strand (5' → 3'); as, antisense strand (5' ← 3').

^b Lowercase letters indicate the sequence added or modified for cloning purposes.

^c The sequences of these primers coincide with the corresponding mouse *Pleiad* sequences and, thus, were also used for amplification of mouse cDNA.

transcripts encoding the conserved C-terminal region of mPLEIADa are expressed in mouse skin cells (Fig. 2d, lanes 6 and 9).

A psi-BLAST homology search of databases using the human PLEIAD (hPLEIAD) sequence as a seed revealed significant conservation of the C-terminal half of hPLEIAD, corresponding approximately to exons 5–12 (hPLEIAD-C), among vertebrates (Fig. 2a and Tables 2 and 3). In contrast, the sequence of the N-terminal half of hPLEIAD, hPLEIAD-N, was not an efficient seed for retrieving a conserved structure among vertebrate PLEIAD homologs. These observations suggest that the regulation of CAPN3 autolysis was conducted by the C-terminal region of PLEIAD homologs during evolution.

PLEIAD interacts with CTBP1, a potential CAPN3 substrate

Yeast two-hybrid (YTH) screening identified CTBP1 as an interacting protein candidate for

PLEIAD. CTBP1 is a highly conserved transcriptional co-repressor, and its structure–function relationships have been well studied (Fig. 3a).³⁴ In addition to hPLEIADa, which was originally used as a bait construct for the screening, hPLEIADf also interacted with CTBP1 (data not shown). In contrast to PLEIAD's effect on CAPN3's autolysis, PLEIAD's N-terminal region was sufficient for its interaction with CTBP1 (Fig. 3b, column D).

To characterize the mechanism of the CTBP1–PLEIAD interaction, we examined mutations that have been shown to abrogate CTBP1's interaction with the PLDLS motif in target proteins (Fig. 3b, columns F and H). Examining two mutants, A52E and V66R, did not demonstrate the interaction with hPLEIADa, hPLEIAD-N, or hPLEIADf:ex4term (2F to 4F and 2H to 4H). Therefore, it is possible that the structure of CTBP1 critical for its formation of co-repressor complexes is also involved in its interaction with PLEIAD. On the other hand, mutations in NAD(H)-binding domain of CTBP1 caused autoactivation of

Table 2. Amino acid sequences of PLEIAD homologs used in this study

Species (abbreviation)	General name	Accession no. ^a	Size (aa)	Homologous region ^b (aa)
<i>Homo sapiens</i> (<i>H. s.</i>)	Human	Q8NDZ2	872	459–872
<i>Mus musculus</i> (<i>M. m.</i>)	Mouse	NP_795961.3	1354	945–1354
<i>Bos taurus</i> (<i>B. t.</i>)	Bovine	XP_002690456.1	451	44–451
<i>M. domestica</i> (<i>M. d.</i>)	Opossum	XP_001380898.1	865	461–865
<i>Gallus gallus</i> (<i>G. g.</i>)	Chicken	XP_414554.1	646	245–646
<i>Taeniopygia guttata</i> (<i>T. g.</i>)	Zebra finch	XP_002194388.1	605	210–605
<i>Meleagris gallopavo</i> (<i>M. g.</i>)	Turkey	XP_003210405.1 ^c (ENSMGAT00000005306)	433	32–433
<i>Anolis carolinensis</i> (<i>A. c.</i>)	Green anole lizard	XP_003227968.1 ^c (ENSACAT00000006428)	441	47–441
<i>Xenopus tropicalis</i> (<i>X. t.</i>)	Western clawed frog	XP_002938112.1 ^c (NW_003163664, ENSXETT000000064005, EL834443)	587	215–587
<i>Oreochromis niloticus</i> (<i>O. n.</i>)	Cichlid fish	XP_003455259.1 ^c (NT_167549)	426	43–426
<i>Tetraodon nigroviridis</i> (<i>T. n.</i>)	Puffer fish	CAF92416 ^{c,d} (CAAE01009900)	316	54–316
<i>Danio rerio</i> (<i>D. r.</i>)	Zebra fish	XP_001922583.1 ^c (ENS DART00000129265)	770	381–770

^a Data were retrieved from NCBI and Ensembl databases.

^b Amino acid sequences corresponding to those encoded by exons 5–12 (459–872) in the human C5orf25 gene were used for analysis.

^c The sequence was revised using genomic and EST sequences shown in parentheses.

^d Gaps were left unfilled in consideration of uncertainty of deposited genome sequences.

Table 3. Identity and similarity among 12 vertebrate PLEIAD sequences

% Identity	Mammals				Birds			Reptile	Amphibian	Fish		
% Similarity	<i>H. s.</i>	<i>M. m.</i>	<i>B. t.</i>	<i>M. d.</i>	<i>G. g.</i>	<i>T. g.</i>	<i>M. g.</i>	<i>A. c.</i>	<i>X. t.</i>	<i>O. n.</i>	<i>T. n.</i> ^a	<i>D. r.</i>
<i>H. s.</i>		93.1	92.9	70.4	51.0	47.2	48.8	46.7	41.2	33.2	<i>43.2</i>	36.1
<i>M. m.</i>	99.0		89.7	70.4	51.0	46.9	50.0	46.2	41.0	33.5	<i>35.9</i>	36.6
<i>B. t.</i>	99.5	99.0		69.4	50.2	46.5	49.5	45.9	40.5	33.5	<i>37.5</i>	36.1
<i>M. d.</i>	91.0	91.5	91.0		50.3	47.3	50.5	44.6	38.4	34.3	<i>38.5</i>	34.5
<i>G. g.</i>	84.4	83.9	84.2	84.5		65.9	91.3	50.6	41.1	33.9	<i>35.8</i>	34.0
<i>T. g.</i>	82.0	82.0	81.8	81.8	90.0		66.8	47.0	40.7	33.3	<i>30.3</i>	35.0
<i>M. g.</i>	82.2	83.2	83.2	83.5	98.0	89.8		49.6	41.4	33.9	<i>37.9</i>	35.0
<i>A. c.</i>	79.7	79.4	78.9	81.0	82.0	80.5	82.5		39.7	31.5	<i>33.9</i>	32.6
<i>X. t.</i>	75.0	75.8	75.3	78.0	76.1	76.7	76.1	75.6		31.3	<i>29.0</i>	30.4
<i>O. n.</i>	73.1	73.4	73.4	72.6	70.8	70.5	72.0	70.8	76.5		<i>46.8</i>	53.2
<i>T. n.</i>	77.3	72.6	77.3	74.0	70.5	68.1	72.6	71.4	71.0	79.9		39.5
<i>D. r.</i>	72.8	73.5	72.0	75.5	73.0	74.1	72.9	74.7	79.3	85.8	<i>81.5</i>	

Species names are abbreviated as in Table 2.

^a The values for the *T. nigroviridis* sequence are shown in italics since this sequence contains three gaps.

the prey plasmid and were not competent for the analysis using YTH system.

Unlike the interaction between CAPN3 and PLEIAD, the interaction between CTBP1 and PLEIAD and/or CAPN3 was not detectable using protein expression in COS7 cells. To ensure the presence of excess amount of CTBP1, we performed *in vitro* cotranslation of PLEIAD and CAPN3:CS in the presence of CTBP1 using cell-free protein expression system (Fig. 3c). Both PLEIADa and PLEIADf together with CTBP1 were coimmunoprecipitated by anti-CAPN3 (Fig. 3d, lanes 5 and 7). In contrast to PLEIAD, the amount of CTBP1 in immunoprecipitate was very small and the efficiency was quite low considering its abundant presence in "Input" (lanes 1–4).

Unexpectedly, the expression of CAPN3:WT in COS7 cells caused a significant decrease in endogenous CTBP1 (Fig. 4a, lane 3, gray arrowhead). This decrease was even more pronounced when the triple-tagged CTBP1 construct, MYC-CTBP1-EGFP-FLAG, was coexpressed with CAPN3:WT (Fig. 4a, lane 1). The detected major proteolytic fragment size (open arrow), ca 35 kDa, was larger than that calculated for EGFP with FLAG, ca 30 kDa, indicating that proteolysis by coexpressed CAPN3 occurred within CTBP1 and not in the tag regions. A splicing variant of mouse CAPN3, CAPN3:ΔIS1,³⁵ also resulted in the proteolysis of coexpressed CTBP1 (Fig. 4b, lane 4). As summarized at the bottom of Fig. 4b, the proteolysis of CTBP1 occurred in parallel with that of other potential CAPN3 substrates identified in COS7 cells, such as calpastatin and fodrin. The C-terminal proteolyzed fragment was purified by anti-FLAG immunoprecipitation, and its N-terminal sequence was determined to be G⁴¹⁰LPPVA by N-terminal sequencing (Fig. 4b, open arrow; data not shown).

We next examined if the proteolysis of endogenous CTBP1 in differentiated mouse skm primary cultured cells was induced upon the activation of CAPN3 by ouabain treatment, which increases the intracellular Na⁺ and (indirectly) Ca²⁺ concentrations.³² The result was under our detection level (Fig. 4c, lane 2), suggesting that, unlike CAPN3 expressed in COS7 cells, substrate proteolysis by endogenous CAPN3 in skm is still tightly regulated even when its autolysis is detectable and/or the proteolysis of endogenous CTBP1 does not occur at a level that is artificially induced by CAPN3 overexpression in COS7 cells.

The effect of missense mutations that have been shown to compromise complex formation activities of CTBP1 on its property as a substrate for CAPN3 was also examined. Except for the mutation A52E, these mutations altered the susceptibility of CTBP1 to CAPN3-mediated proteolysis while the decrease in the amount of the proteolyzed fragment was observed.

These results suggest that PLEIAD has at least two functions mediated by different regions of the molecule: the N-terminal region recruits CTBP1, a substrate for CAPN3, and the C-terminal region is involved in suppressing CAPN3's protease activity.

CTBP1 is also a substrate for conventional calpains

To obtain insight into the role of calpains in the proteolysis of CTBP1, we examined the proteolysis of recombinant CTBP1 by recombinant conventional calpains *in vitro*. CTBP1 was proteolyzed by CAPN1 + CAPNS1 (also called μ-calpain, abbreviated as "CAPN1/S1" in Fig. 5a, lanes 3 and 4) and CAPN2/S1 (m-calpain; data not shown). The specificity of the reaction was shown by the suppression

of most of the proteolysis in the presence of calpastatin (Fig. 5a, lane 5) or in the absence of Ca²⁺ (lane 6). In parallel, reactions carried out in the

presence (sample in lane 4) or absence (sample in lane 6) of Ca²⁺ were analyzed by mass spectrometry to determine the sequences of proteolyzed

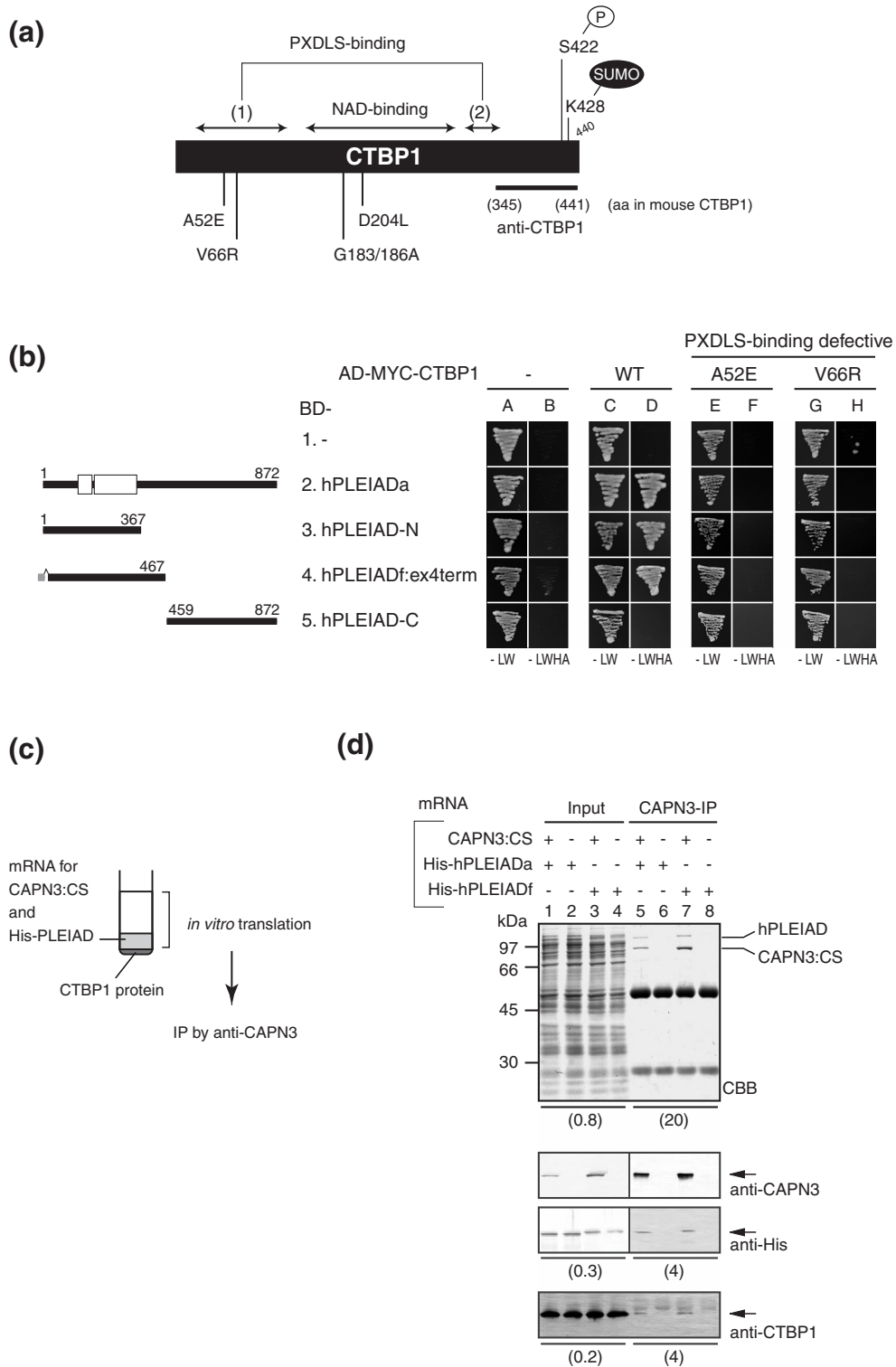


Fig. 3 (legend on next page)

fragments. With >99% confidence, four peptides were identified in the [+Ca²⁺] sample [Fig. 5b, (i) to (iv)], two of which [Fig. 5b, (iii) and (iv)] were also detectable in the [-Ca²⁺] sample. These findings suggested that CTBP1 is cleaved at the N-termini of G376 (Fig. 5b, [1]) and V388 (Fig. 5b, [2]) by CAPN1 + S1 in the presence of Ca²⁺.

As mentioned above, CAPN3 proteolyzed CTBP1 at Gly410 at the N-terminus (Fig. 4c). Therefore, the same position detected here (Fig. 5b, [4]) is very likely to be a proteolytic site for conventional calpain, as well. However, the possibility of nonspecific proteolysis by non-calpain contaminating proteases cannot be completely eliminated due to the detection of the same peptides in the [-Ca²⁺] sample, although their intensity was much lower than that detected in the [+Ca²⁺] sample. In addition, analysis of the CTBP1 sequence using our cleavage site predictor for calpain³⁶ recognized the three positions [1], [2], and [4] by three different algorithms (Fig. 5c). Collectively, these data indicate that sites [1], [2], and [4] are probably cleaved by conventional calpain and that site [3] may represent nonspecific proteolysis. It remains unclear whether cleavage sites [1] and [2] are recognized by CAPN3. However, the small amount of a fragment detectable above the major proteolyzed fragments in Fig. 4b (lanes 2 and 4, gray arrow) may indicate that the cleavage by CAPN3 also occurred at sites [1] and/or [2].

PLEIAD may regulate CAPN3 that is not bound to sarcomere components

To gain further insight into PLEIAD's physiological relevance, we examined PLEIAD's cellular localization in primary cultures of chick skeletal myotubes expressing EGFP-hPLEIADf (Fig. 6). In total, 200 transfected cells expressing EGFP-hPLEIADf were compared to 150 cells expressing EGFP alone. In ~10% of the transfected cells, hPLEIADf was localized in a striated pattern within the sarcomeric I band, but most cells showed diffuse cytoplasmic staining (Fig. 6d, inset: see GFP staining, i.e., hPLEIADf, on each side of the Z-line, marked by

staining for α -actinin). These results suggested that PLEIAD's primary target may be a population of CAPN3 that exists in the cytosol. For unknown reasons, it was more difficult to express EGFP-hPLEIADa as efficiently as EGFP-hPLEIADf. These two isoforms also showed different expression/degradation patterns in COS7 cells, independent of CAPN3's protease activity (Fig. 1d, lanes 4 and 5 and lanes 8 and 9, anti-FLAG). Such a difference might be enhanced in skeletal myotubes, resulting in a more severe degradation of hPLEIADa than of hPLEIADf.

Discussion

The unique properties of CAPN3 include its very rapid and exhaustive autolysis *in vitro* in protein expression systems and nonmuscle cultured cells (CAPN3 is stable in primary skm cells²¹) and its dependence on both Na⁺ and Ca²⁺ for its activation.³² These phenomena have been studied mostly with respect to causative factors; for example, it has been shown that CAPN3-specific insertion sequences, IS1 and IS2, are required for autolytic events.^{21,35,37} In contrast, it is unclear why CAPN3 remains intact in skm cells without undergoing autolysis. Surprisingly, in CAPN3:CS knockin mice, in which the endogenous wild-type CAPN3 (CAPN3:WT) is replaced by a protease-inactive mutant CAPN3:CS, the amount of CAPN3:CS protein detected in the skm cells and tissues is the same as in wild-type mice. Moreover, the presence of intact CAPN3 protein, that is, of either WT or the CS mutant, is sufficient to fulfill its function at the triad region, even when its protease activity is lacking.^{18,19} These findings strongly suggest that, in addition to connectin/titin, which is a strong candidate for stabilizing and regulating CAPN3 in muscle sarcomeres, another mechanism is present to stabilize CAPN3, especially when it is not associated with sarcomeres.

As an approach to understanding the mechanism by which CAPN3 conducts diverse functions in

Fig. 3. The N-terminal region of PLEIAD interacts with CTBP1. (a) YTH screening using a human skm cDNA library identified CTBP1 as a binding protein for PLEIAD. The functional annotation for human CTBP1 is shown. Among previously validated missense mutants, four different mutants that compromised complex formation activities of CTBP1 were selected. The mouse sequence has an insertion of 1 aa at the C-terminal region and therefore consists of 441 aa. Horizontal bar indicates the antigenic polypeptides for anti-CTBP1. (b) The N-terminal region, hPLEIAD-N or hPLEIADf:ex4term, was sufficient for the interaction (3D and 4D), while the C-terminal region, hPLEIAD-C, shared by both hPLEIADa and f, failed to undergo detectable interaction (5D). Two different mutations in PXDLS-binding domain of CTBP1 showed negative effect on its interaction with PLEIAD (2F to 4F and 2H to 4H). (c) Complex formation of CAPN3, PLEIAD, and CTBP1 was examined using wheat-germ cell-free expression system. In addition to the layer of mRNA and other components for translation reaction, solution of CTBP1 protein was set on the bottom of the tube. After translation, layers were mixed and subjected to immunoprecipitation using anti-CAPN3 antibody. (d) Both PLEIADa and PLEIADf were coimmunoprecipitated with CAPN3:CS (lanes 5 and 7, CBB and anti-His). In these samples, CTBP1 was also detected (anti-CTBP1). Numbers in parentheses indicate the percentage of the total amount. Nonspecific degradation or precipitation of CTBP1 during translation reaction was not detected (data not shown).

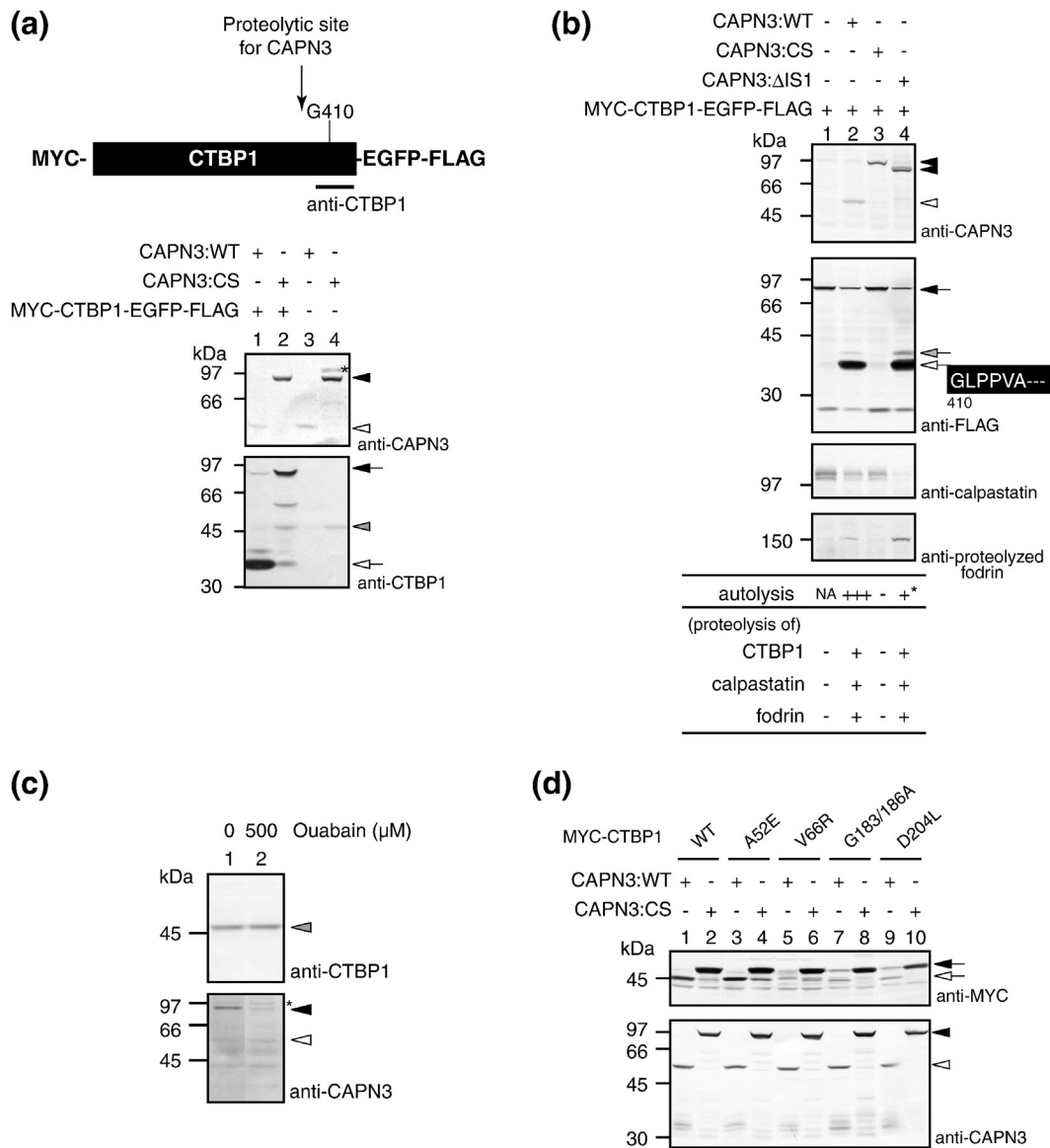


Fig. 4. CTBP1, a binding protein for PLEIAD, is a potential CAPN3 substrate. (a) Triple-tagged CTBP1 (MYC-CTBP1-EGFP-FLAG) expressed in COS7 cells was proteolyzed when CAPN3:WT was coexpressed (lane 1). This CTBP1 construct was susceptible to proteolysis (lane 2), but the difference between lanes 1 and 2 was still significant. In the cells expressing CAPN3:WT, the endogenous CTBP1 was undetectable (compare lanes 3 and 4). (b) Proteolysis of the CTBP1 construct was also observed in COS7 cells coexpressing mouse CAPN3:ΔIS1 (lane 4, anti-FLAG); CAPN3:ΔIS1 is a splicing variant that shows protease activity comparable to that of WT but lacks the autolytic sites encoded by exon 6. The C-terminal proteolyzed fragment of the CTBP1 construct was immunoprecipitated by anti-FLAG, and its N-terminal sequence was determined. (c) In cultured myotubes, the activation of CAPN3 by ouabain treatment did not cause significant proteolysis of endogenous CTBP1 protein (lane 2). (d) Proteolysis of CTBP1 by CAPN3 depends on functional structure of CTBP1. Four different CTBP1 mutants (see Fig. 3a) were coexpressed with CAPN3:WT or CAPN3:CS. In contrast to wild-type CTBP1, three of the mutants showed altered susceptibility to proteolysis (lanes 5, 7, and 9). For the mutant A52E, no significant change was observed (lane 3). Closed and open arrowheads indicate the full-length and autolytic fragments of CAPN3, respectively, detected by Western blotting using an anti-CAPN3 antibody. Gray arrowheads indicate endogenous CTBP1. Closed, open, and gray arrows indicate the full-length, the main, and the minor proteolyzed fragment of the CTBP1 construct expressed in COS7 cells, respectively.

different subcellular compartments, we sought to identify molecular interactions that affect its protease activity. Here, we showed that PLEIAD/SIMC1/

C5orf25, a novel CAPN3-binding protein, moderates the protease activity of CAPN3 and possesses the potential to function as a scaffold protein.

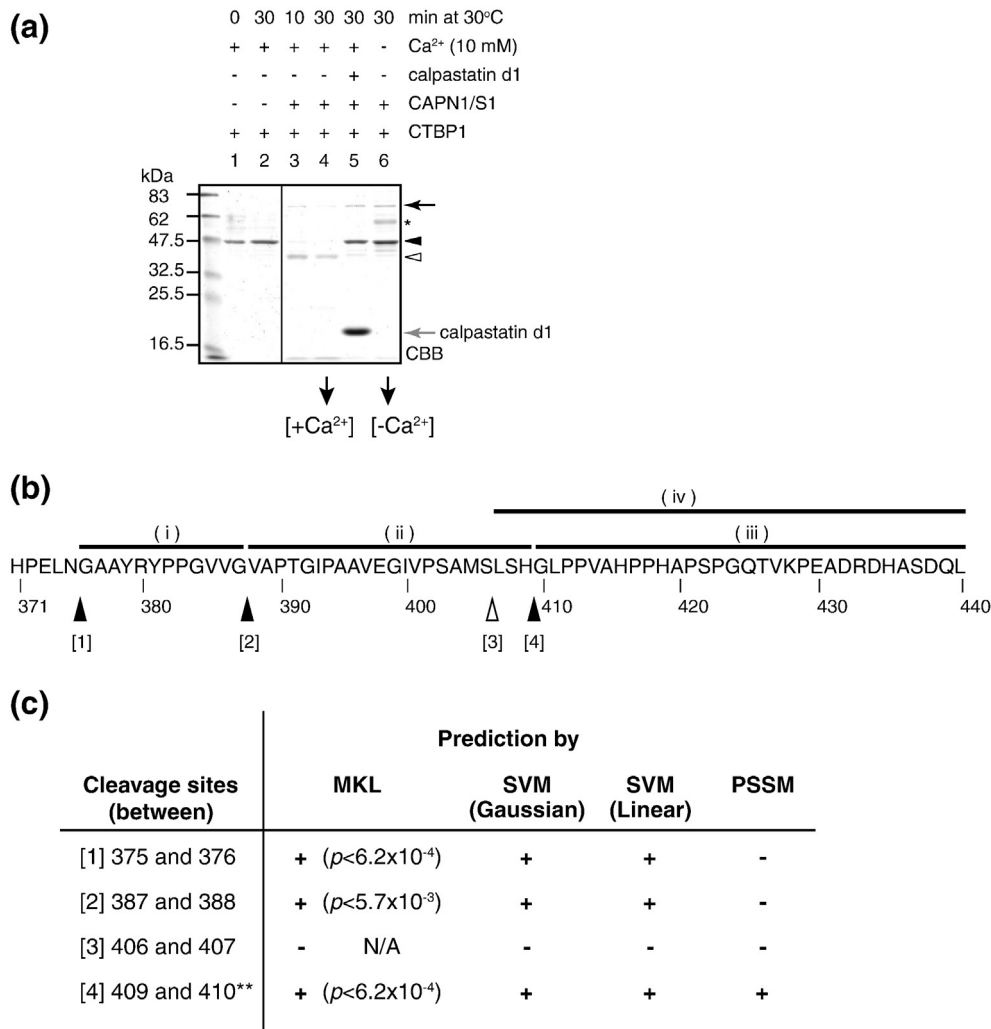


Fig. 5. Proteolysis of CTBP1 by classical calpain, μ -calpain (CAPN1/S1), revealed additional cleavage sites. (a) Recombinant CTBP1 protein was incubated under the conditions indicated at the top. CTBP1 was proteolyzed by CAPN1/S1 in the presence of Ca²⁺ (lane 4), and this reaction was inhibited by calpastatin peptide (lane 5). Peptide fractions generated in the presence (lane 4, [+Ca²⁺]) or in the absence (lane 6, [-Ca²⁺]) of Ca²⁺ were further analyzed by mass spectrometry. Closed and open arrowheads indicate the full-length and the main proteolyzed fragment of recombinant CTBP1. Closed and open arrows indicate CAPN1 and recombinant calpastatin domain 1. *, unidentified signal. (b) Four peptides were identified in the [+Ca²⁺] sample [horizontal bars (i) to (iv)], and four cleavage sites by CAPN1/S1 at the C-terminus of CTBP1 were revealed (vertical arrowheads, [1] to [4]). Two sequences, (iii) and (iv), were also detected in the [-Ca²⁺] sample, suggesting that the peptide bonds at positions [3] and [4] have a propensity to be hydrolyzed. (c) Calpain cleavage sites in CTBP1 were predicted using our predictor available at <http://www.calpain.org>. Three cleavage sites, [1], [2], and [4], coincided with those predicted by at least three different algorithms. +, predicted; -, not predicted; **, biochemically identified as the cleavage site for CAPN3 [Fig. 4, (c)].

PLEIAD is a novel CAPN3-regulating protein

So far, this is the first report on the functional properties of PLEIAD. In addition, we have shown that, in skm, a *Pleiad* transcript that lacks exons 2 and 3 is the predominant variant. Notably, this PLEIAD variant has not been identified in other human tissues, such as brain or testis, strongly suggesting that it is a low-abundance isoform that may be muscle specific. Unlike CAPN3, the ubiqui-

tous expression of PLEIAD has been shown in databases at both transcript[†] and protein levels.[‡] The differential expression of PLEIAD has been detected by the transcriptional profiling of many diseases, including muscular dystrophies,³⁸ but it is not clear if these changes are related to CAPN3's functions. YTH screening revealed that PLEIAD also interacts with CTBP1, and it may interact with other cytosolic and/or cytoskeletal proteins. Therefore, further studies are necessary to address the

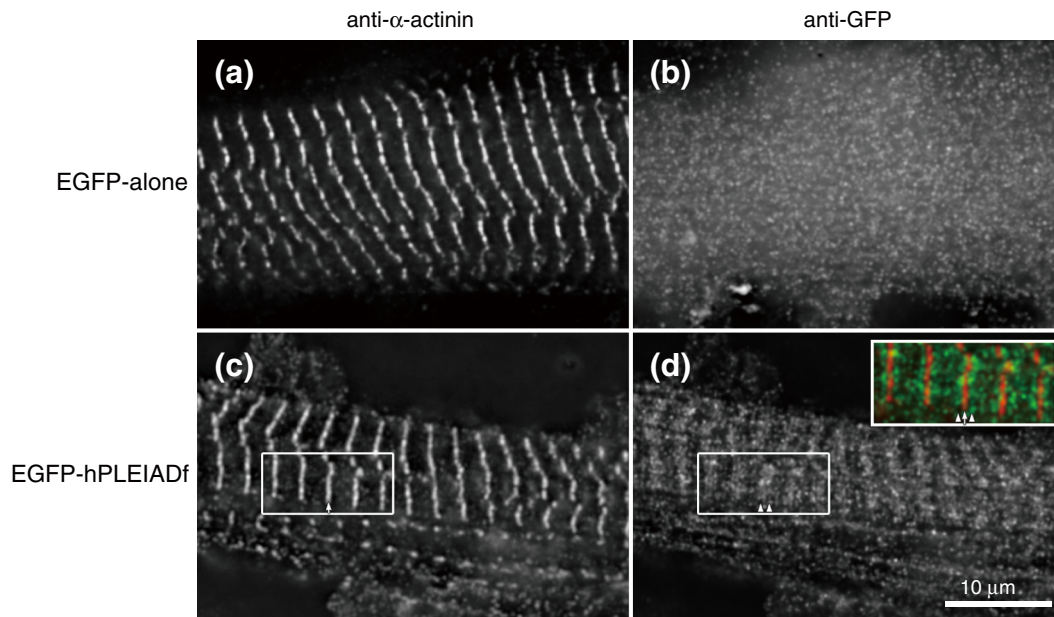


Fig. 6. PLEIAD shows diffuse cytoplasmic localization in skeletal myotubes. Localization of expressed EGFP-hPLEIADf was examined in cultured chick skeletal myotubes. Cells were stained with anti-sarcomeric α -actinin (a and d) and anti-GFP antibodies (b and d). The primary localization of hPLEIADf was diffusely cytoplasmic (data not shown). Occasionally, in about 10% of transfected cells, EGFP-hPLEIADf was localized in a striated pattern within the sarcomeric I band, on each side of the Z-line (d, inset). Arrow and arrowheads indicate a Z-line labeled by α -actinin and EGFP-hPLEIADf, respectively. The scale bar represents 10 μ m.

possibility that PLEIAD has many functional links to other proteins, not only in skm but also in other tissues. The two recently identified tandem SUMO-interacting motifs at PLEIAD's N-terminus also indicate its potential roles in signaling pathways regulated by sumoylation. Another interesting finding is that humans have one PLEIAD pseudogene (*PLEIAD-ps1*, originally called *LOC202181*) close to *PLEIAD* (5q35.3 and 5q35.2, respectively).

From the viewpoint of molecular evolution, it is noteworthy that the C-terminal region of PLEIAD, which is responsible for the CAPN3 suppressor effect, is significantly conserved from human to fish and that CAPN3 is also evolutionarily conserved among vertebrates. There are, however, some inconsistencies: (1) The mouse ortholog, mPLEIAD, is much larger than the orthologs found in most mammals. The observed increase in protein size is caused by the insertion of a highly repetitive sequence in mouse exon 2, which corresponds to human exon 4. (2) At least in human and in mouse, one splicing variant has a structurally identical exon composition, and this variant lacks exon 4 in the human and exon 2 in the mouse [Figs. 1b, (c: Δ ex2-4) and 2c, (b)], respectively. Although these variants were not detected in skm in our hands, the identified transcripts in lower vertebrates show more similarity to these variants and lack the N-terminal region. (3) The ortholog found in marsupials, *Monodelphis*

domestica (opossum), lacks the sequence corresponding to the Pro-rich region in hPLEIAD [Fig. 2a, (4)].³⁹ It is a serious concern that potential sequencing errors in databases could result in our misinterpretation of the structure of PLEIAD homologs, while our sequence analyses suggested that the PLEIAD gene has been a target of evolutionary modification by repetitive sequences, such as transposable elements.⁴⁰ These findings complicate our conclusion regarding the canonical functional structure of PLEIAD. In particular, the second point described above argues against the simple explanation that the N-terminal region of PLEIAD recruits substrates while its C-terminal region suppresses the CAPN3 protease activity. It is possible that the CAPN3-suppressing activity was conserved during vertebrate evolution, whereas the functions of the N-terminal parts diverged. It is nonetheless tempting to speculate that the N-terminal substrate scaffold function is applicable to the PLEIAD orthologs found in large mammals such as human and bovines.

Relevance of the C-terminal cleavage in CTBP1 functions

Our biochemical evidence indicated that CTBP1 is a good substrate for calpains including CAPN3. CTBP1 has multiple functions in both the nucleus and the cytoplasm.^{30,31,41,42} In particular, its function

as a nuclear transcriptional regulator has been well studied.^{43–45} CTBP1's regulation is important for proper proliferation and differentiation.^{45–49} For example, the down-regulation of CTBP1 at the protein level, which is catalyzed by the ubiquitin-proteasome pathway,⁵⁰ counteracts oncogenic gene expression.⁵¹ In addition, phosphorylation and sumoylation at the C-terminus of CTBP1 exert regulatory effects.⁴² Notably, CTBP1's cleavage by calpains removes these modification sites, suggesting that calpains also participate in the regulation of CTBP1, although we could not detect this cleavage *in vivo*.

The function of CTBP1 in skm remains unclear; therefore, it is difficult to speculate about what the outcomes of CAPN3-mediated CTBP1 proteolysis are. One possibility is that the regulation of CTBP1 by CAPN3 is functionally analogous to a previously proposed role of CAPN3 in down-regulating β -catenin in skm.¹³ Since CTBP1 itself is capable of carrying out multi-directional functions, its stage-specific regulation may be involved in skm cell fusion and development into myotubes.

For the interaction between CTBP1 and PLEIAD, it was suggested that PxDLS-binding site on CTBP1 is involved at the level of YTH assay, and further analyses are required to evaluate its biological significance. It was also suggested that CAPN3 recognizes the structure of CTBP1 relevant for its PxDLS binding and NAD(H) binding. However, there is a possibility that the selected CTBP1 mutations have too strong effect on the overall structure of the molecule and the essential structure of CTBP1 as a substrate for calpain warrants further investigation.

Possible link between the CAPN3–PLEIAD and CAPN3–connectin/titin interactions

We previously proposed that the N2A region of connectin/titin supports the functions of CAPN3 by stabilizing CAPN3 while it recruits MARPs (*muscle ankyrin repeat proteins*) as substrates for CAPN3. Such a model is physically possible for connectin/titin, since it is located in sarcomeres, which are mostly composed of extension-competent structures, such as immunoglobulin motifs and fibronectin type III-like domains. From the primary sequence of PLEIAD, it is not clear if a robust structural change occurs upon its interaction with CAPN3 and/or CTBP1. Still, it is worth noting that the C-terminal functional region of PLEIAD has no defined structure and/or motif. The specificity and efficiency of calpastatin, a specific inhibitory protein for classical calpains except CAPN3, relies on its unstructured nature; it is classified as an intrinsically unstructured/disordered protein⁵²; calpastatin binds close to, but loops out into, the side opposite calpain's active site, escaping cleavage by the calpain.^{53,54} Although there is not a strong sequence similarity between

PLEIAD and calpastatin, it is possible that PLEIAD functions in an analogous manner. We also hypothesize that the N-terminal region of PLEIAD is involved in the regulation of CAPN3 autolysis by increasing the affinity of the molecule to the full-length, pre-autolyzed form of CAPN3 but is susceptible to protease activity of CAPN3. On the other hand, the C-terminal region of PLEIAD is resistant to protease activity of CAPN3 but has lower ability to interact with CAPN3 by its own.

We sought to detect endogenous mPLEIAD in mouse tissues using two commercially available anti-hPLEIAD antibodies. These antibodies did not yield consistent results; thus, we suspended our analysis of mouse PLEIAD localization during the preparation of this manuscript. Instead, we used an alternative approach, the expression of hPLEIAD in chicken primary cultured skeletal myotubes. The localization of expressed hPLEIADf (see Fig. 6) showed that this new regulator of CAPN3 is primarily distributed diffusely in the cytoplasm. At the same time, the occasional localization of hPLEIADf within the sarcomeric I-band region raises the intriguing possibility that connectin/titin and PLEIAD cooperate as CAPN3 regulators. Further investigation of the spatiotemporal expression of the PLEIAD protein in skm is required in order to address this issue.

In this study, a novel protein–protein interaction that is capable of regulating CAPN3 in the cytoplasm as well as in the sarcomere was shown. Along with the identification of possible CAPN3 functions in different cellular compartments, it has been unknown how CAPN3 avoids autolytic degradation while it is translocated. We anticipate that the present study will serve as a good starting point toward understanding how CAPN3 conducts its multiple functions. It is likely that there are other interacting molecules relevant to CAPN3's functions that are yet to be discovered.

Materials and Methods

Experimental animals

All procedures used for experimental animals were approved by the Experimental Animal Care and Use Committee of Tokyo Metropolitan Institute of Medical Science, and the animals and related materials were treated in accordance with the committee's guidelines.

cDNA constructs

The cDNA clone for PLEIAD/C5orf25, which was originally purchased from Ressourcenzentrum Primärdatenbank (German Science Centre for Genome Research), is now available from Source BioScience (IRATp970H0629D). The cDNAs for human CAPN3 and mouse CAPN3 Δ 1 were subcloned into the pSRD expression vector for

protein expression in mammalian cells, as described previously.^{25,35} These cDNAs were also expressed as N-terminal FLAG-tagged or MYC-tagged proteins using the pSRD or pcDNA3.1 expression vector (Invitrogen, Grand Island, NY).⁵⁵ The pEGFP-C1 expression vector was also used. For the YTH assay, the pAS2-1c²⁵ and pACT2 expression vectors (U29899; Clontech, Mountain View, CA) were used. Enzymes used to manipulate recombinant DNA were purchased from Takara Bio (Shiga, Japan) or New England Biolabs (Ipswich, MA). The mutations described here were introduced by long PCR using *Pfu*-Turbo DNA polymerase, as described previously.⁵⁶ All the constructs were verified by DNA sequencing.

PCR and RT-PCR analyses

Endpoint PCR reactions to detect the expression of C5orf25 were performed using ExTaq DNA polymerase (Takara) and the appropriate primer pairs (Fig. 1b and Table 1). Some PCR products were sequenced for verification. The human skm cDNA library for YTH (Clontech) or mouse skm cDNA synthesized from total RNA was used as a template. Total RNA was prepared from cultured mouse muscle cells and the quadriceps femoris of 30-week-old C57BL/6J mice using TRIzol® Reagent (Invitrogen), according to the manufacturer's instructions. For RT by PrimeScript® Reverse Transcriptase (Takara), 1.5 µg and 1.1 µg of total RNA from cultured cells and tissues, respectively, were used per 10-µl reaction.

Cell culture and protein expression

Protein expression in HEK293 cells was performed as previously described.²⁸ COS7 cells were grown in Dulbecco's modified Eagle's medium (Sigma-Aldrich, St. Louis, MO) supplemented with 10% fetal bovine serum that had been heat inactivated at 56 °C for 30 min before use. For recombinant protein expression in COS7 cells, the plasmid was prepared at a concentration of 1 µg/µl and transfected using TransIT®-LT1 (Mirus Bio LLC, Madison, WI). As a standard, 2–4 µg of plasmid plus a 3× volume of transfection reagent were used per 1.5×10^5 cells plated in 3.5-cm dish, 12–16 h prior to transfection. The cells were harvested 40–60 h after transfection using ice-cold phosphate-buffered saline.²⁶

Primary cultures of chick skeletal myotubes were prepared as described previously.⁵⁷ Cells used for immunofluorescence were grown on coverslips coated with Matrigel™ (BD Biosciences, San Jose, CA) diluted to 0.5 mg/ml in minimum essential medium. Transfection was performed 12–16 h after plating using Effectene (Qiagen, Valencia, CA), as previously described.⁵⁸ Primary cultures of mouse skm cells were prepared as described previously.²⁷ Cells were allowed to differentiate for 5 and 10 days and used for total RNA purification and a 2-h incubation with ouabain, respectively.

In vitro transcription and translation were performed using a wheat-germ cell-free expression system, according to the manufacturer's instructions (CellFree Sciences, Japan). The mRNAs for each construct were transcribed separately. The translation reaction was carried out at

16 °C for 18–20 h without shaking. Two micrograms of recombinant CTBP1 (1 mg/ml stock solution) was added to the bottom of 112-µl translation reaction mixture.

Immunoprecipitation

Harvested cells were suspended in lysis buffer [50 mM Tris–HCl (pH 7.5), 150 mM CsCl, 1 mM ethylenediaminetetraacetic acid–KOH (pH 8.0), and 1% Triton X-100] containing protease inhibitors [1 mM 4-(2-aminoethyl) benzenesulfonyl fluoride hydrochloride, 0.1 mM leupeptin, 10 µg/ml aprotinin, and 10 mM iodoacetamide] and incubated on ice for 30 min with occasional mixing. The supernatant was collected after centrifugation at 20,630g at 4 °C for 15 min. Incubation with anti-FLAG M2 affinity gel (Sigma-Aldrich) and elution of the immunoprecipitated proteins were performed according to the manufacturer's instructions using a modified wash buffer [50 mM Tris–HCl (pH 7.5) and 150 mM CsCl].²⁶ To detect the CAPN3–PLEIAD interaction, we carried out the incubation for 2–3 h. When anti-CAPN3 antibody was used for immunoprecipitation, the immunocomplex was recovered by Protein-G Sepharose (GE Healthcare). The eluate was subjected to SDS-PAGE and Western blot analysis. For N-terminal sequencing, the immunoprecipitated proteins were blotted onto a ProBlott membrane (Applied Biosystems, Carlsbad, CA) after SDS-PAGE. The target protein bands were visualized by CBB G-250 staining, excised, and submitted to APRO Science Institute Inc. (Tokushima, Japan) for sequence analysis.

Western blot analysis

Proteins were separated by SDS-PAGE and transferred onto polyvinylidene fluoride membranes (Millipore, Bedford, MA). The membranes were probed with the appropriate primary antibodies and horseradish-peroxidase-coupled secondary antibodies (Nichirei, Tokyo, Japan) followed by visualization using a POD immunostaining kit (Wako, Osaka, Japan) or SuperSignal® West Pico Chemiluminescent Substrate (Pierce, Rockford, IL).²⁶ Scanned images were processed for presentation using Adobe Photoshop CS6 (Adobe Systems, San Jose, CA).

Immunofluorescence analysis

Immunofluorescence microscopy was performed as described previously.⁵⁸ At 4–5 days after transfection, the cells were incubated in relaxing buffer [150 mM KCl, 5 mM MgCl₂, 10 mM 3-(*N*-morpholino) propanesulfonic acid (pH 7.4), 1 mM ethylene glycol bis(β-aminoethyl ether) *N,N*-tetraacetic acid, and 4 mM ATP] for 15 min, followed by fixation using 2% formaldehyde in relaxing buffer for 15 min. The primary and secondary antibodies were used at the concentrations described in [Antibodies](#). Coverslips were mounted onto slides with Aqua Poly/Mount (Polysciences, Warrington, PA), and the samples were analyzed on an Axiocvert microscope (Zeiss, Oberkochen, Germany) using 63× (NA 1.4) or 100× (NA 1.3) objectives. The cells were also analyzed using a Deltavision RT system (Applied Precision, Issaquah, WA) with an inverted microscope (IS70; Olympus, Tokyo, Japan), a

100× (NA 1.3) objective, and a charge-coupled device camera (CoolSNAP HQ; Photometrics, Huntington Beach, CA). The images were deconvolved using SoftWoRx 3.5.1 software (Applied Precision) and processed for presentation using Adobe Photoshop CS6 (Adobe Systems).

Antibodies

The antibodies used in this study include anti-FLAG mouse monoclonal (1:1000, M2; Stratagene, La Jolla, CA), anti-MYC mouse monoclonal (1:1000, 9E10; Developmental Studies Hybridoma Bank), anti-calpastatin mouse monoclonal (1:1000, PI-11; American Type Culture Collection), anti-CTBP1 mouse monoclonal (1:1000, 3/CtBP1; BD Transduction Laboratories™), anti- α -actinin mouse monoclonal (1:2000, EA-53; Sigma-Aldrich), anti-GFP rabbit polyclonal (1:2000; Abcam, Cambridge, MA), anti-CAPN3 goat polyclonal (1:1000; Cosmo Bio, Tokyo, Japan), anti-His mouse monoclonal (1:2000; Novagen), and anti-proteolyzed fodrin (anti-GMMPR) rabbit polyclonal (1:1000, anti-GMMPR) antibodies.^{26,32} As secondary antibodies, Alexa Fluor 488-conjugated goat anti-rabbit IgG (1:1000; Invitrogen) and Texas Red-conjugated donkey anti-mouse IgG (1:600; Jackson Immunoresearch Laboratories, West Grove, PA) antibodies were used.

Protein identification by mass spectrometry

The FLAG-immunoprecipitates from HEK293 cells were analyzed using direct nanoflow liquid chromatography coupled with tandem mass spectrometry.²⁸ To identify the peptide sequence generated during the *in vitro* proteolysis of CTBP1, we desalted the reaction solution using ZipTip® Pipette Tips (Millipore), and tandem mass spectrometry spectra were acquired by a 4800 MALDI TOF/TOF™ analyzer (AB SCIEX, Framingham, MA). Data were analyzed by Protein Pilot™ software (version 4.5) (AB SCIEX).

Calpain cleavage assay *in vitro*

Two hundred nanograms of recombinant human CTBP1 (ProSpec, Ness Ziona, Israel) was incubated with 25 ng of recombinant human CAPN1/S1 (μ -calpain) (BioVision, Milpitas, CA) in 10 μ l of incubation buffer [20 mM Tris-HCl (pH 8.0), 1 mM ethylenediaminetetraacetic acid-KOH (pH 8.0), and 1 mM DTT] with or without 10 mM CaCl₂ at 30 °C for 10 and 30 min. Where indicated, recombinant human calpastatin domain I (Takara) was added to a concentration of 29 mM. The reaction was stopped by the addition of SDS sample buffer, and the sample was subjected to SDS-PAGE followed by CBB G-250 staining.

YTH assay

Proteins interacting with C5orf25 were screened as previously reported²² using *Saccharomyces cerevisiae* strain AH109. The full-length PLEIAD cDNA cloned into pAS2-1c was coexpressed in the yeast with approximately 1.3×10^6 of a human skm cDNA library in the

pGAD424 vector (Clontech). The plasmids were rescued from colonies grown on SD medium that lacked Leu, Trp, His, and Ade (SD-LWHA) and were sequenced. The rescued plasmids were retransformed with a series of PLEIAD mutants using the Fast™-Yeast Transformation Kit (G-Biosciences/Genotech, St. Louis, MO), according to the manufacturer's instructions. Cotransformants were selected on SD-LW plates, and the expressions of reporter genes were assessed by growth on SD-LWHA plates.

Sequence analysis

Sequence data were retrieved from the NCBI[§] and Ensembl^{||} databases. The sequences from UniProtKB^{||} were also used to check the consistency. BLAST searches were performed with psi-BLAST and BLAST-p and tBLAST-n *versus* the nonredundant protein or nucleotide databases. For phylogenetic analysis, sequences were aligned using MAFFT^{a59} and converted to an unrooted tree diagram after manual inspection. The identity and similarity of aligned sequences were calculated using Genetyx (version 11) (Genetyx Co., Tokyo, Japan). Sequence repeats were identified with RADAR,^{b60} and designated sequences were aligned using MAFFT and Genetyx. To predict calpain cleavage sites, we analyzed the protein sequences with an online cleavage site predictor.^{c7,36,61}

Acknowledgements

We thank all the Calpain Project laboratory members for their invaluable support. This work was supported in part by Japan Society for the Promotion of Science Grants-in-Aid for Scientific Research, 20370055 and 23247021 (to H.S.) and 22770139 (to Y.O.); a Takeda Science Foundation research grant (to H.S.); the Collaborative Research Program of the Institute for Chemical Research; Kyoto University, grant 2010-15 (to H.S.) and grants 2011-18 and 2012-30 (to Y.O.); Toray Science and Technology Grant (to Y.O.); American Heart Association Pre-Doctoral Fellowship 12PRE11900038 (to S.M.N.); and National Institutes of Health Grants HL083146 and HL108625 (to C.C.G.).

Received 30 January 2013;

Received in revised form 28 April 2013;

Accepted 15 May 2013

Available online 21 May 2013

Keywords:

calpain;
skeletal muscle;
autolysis;
scaffold;
substrate

Present address: S. Iemura, Innovative Drug Development Translational Research Section, Fukushima Medical University, 1 Hikariga-oka, Fukushima City, Fukushima Prefecture 960-1295, Japan.

†For example, see <http://www.ebi.ac.uk/gxa/gene/ENSG00000170085>.

‡For example, see <http://www.ebi.ac.uk/pride/searchSummary.do?queryTypeSelected=identification%20accession%20number&identificationAccessionNumber=Q8NDZ2>.
§<http://www.ncbi.nlm.nih.gov/>
||<http://ensembl.org/>
¶<http://www.uniprot.org/>
^a<http://www.genome.jp/tools/mafft/>
^b<http://www.ebi.ac.uk/Tools/pfa/>
^c<http://calpain.org/>

Abbreviations used:

NCBI, National Center for Biotechnology Information;
YTH, yeast two-hybrid.

References

- Sorimachi, H., Imajoh-Ohmi, S., Emori, Y., Kawasaki, H., Ohno, S., Minami, Y. & Suzuki, K. (1989). Molecular cloning of a novel mammalian calcium-dependent protease distinct from both m- and mu-types. Specific expression of the mRNA in skeletal muscle. *J. Biol. Chem.* **264**, 20106–20111.
- Goll, D. E., Thompson, V. F., Li, H., Wei, W. & Cong, J. (2003). The calpain system. *Physiol. Rev.* **83**, 731–801.
- Liu, J., Liu, M. C. & Wang, K. K. (2008). Calpain in the CNS: from synaptic function to neurotoxicity. *Sci. Signaling*, **1**, re1.
- Sorimachi, H., Hata, S. & Ono, Y. (2011). Calpain chronicle—an enzyme family under multidisciplinary characterization. *Proc. Jpn. Acad., Ser. B*, **87**, 287–327.
- Sorimachi, H., Hata, S. & Ono, Y. (2011). Impact of genetic insights into calpain biology. *J. Biochem.* **150**, 23–37.
- Ono, Y. & Sorimachi, H. (2012). Calpains: an elaborate proteolytic system. *Biochim. Biophys. Acta*, **1824**, 224–236.
- Sorimachi, H., Mamitsuka, H. & Ono, Y. (2012). Understanding the substrate specificity of conventional calpains. *Biol. Chem.* **393**, 853–871.
- Richard, I., Broux, O., Allamand, V., Fougerousse, F., Chiannikulchai, N., Bourg, N. *et al.* (1995). Mutations in the proteolytic enzyme calpain 3 cause limb-girdle muscular dystrophy type 2A. *Cell*, **81**, 27–40.
- Beckmann, J. S. & Spencer, M. (2008). Calpain 3, the “gatekeeper” of proper sarcomere assembly, turnover and maintenance. *Neuromuscular Disord.* **18**, 913–921.
- Richard, I., Roudaut, C., Marchand, S., Baghdiguiian, S., Herasse, M., Stockholm, D. *et al.* (2000). Loss of calpain 3 proteolytic activity leads to muscular dystrophy and to apoptosis-associated I κ B α /nuclear factor κ B pathway perturbation in mice. *J. Cell Biol.* **151**, 1583–1590.
- Fougerousse, F., Gonin, P., Durand, M., Richard, I. & Raymackers, J. M. (2003). Force impairment in calpain 3-deficient mice is not correlated with mechanical disruption. *Muscle Nerve*, **27**, 616–623.
- Kramerova, I., Kudryashova, E., Tidball, J. G. & Spencer, M. J. (2004). Null mutation of calpain 3 (p94) in mice causes abnormal sarcomere formation *in vivo* and *in vitro*. *Hum. Mol. Genet.* **13**, 1373–1388.
- Kramerova, I., Kudryashova, E., Wu, B. & Spencer, M. J. (2006). Regulation of the M-cadherin- β -catenin complex by calpain 3 during terminal stages of myogenic differentiation. *Mol. Cell Biol.* **26**, 8437–8447.
- Kramerova, I., Kudryashova, E., Wu, B., Ottenheijm, C., Granzier, H. & Spencer, M. J. (2008). Novel role of calpain-3 in the triad-associated protein complex regulating calcium release in skeletal muscle. *Hum. Mol. Genet.* **17**, 3271–3280.
- Kramerova, I., Kudryashova, E., Wu, B., Germain, S., Vandenborne, K., Romain, N. *et al.* (2009). Mitochondrial abnormalities, energy deficit and oxidative stress are features of calpain 3 deficiency in skeletal muscle. *Hum. Mol. Genet.* **18**, 3194–3205.
- Kramerova, I., Kudryashova, E., Ermolova, N., Saenz, A., Jaka, O., Lopez de Munain, A. & Spencer, M. J. (2012). Impaired calcium calmodulin kinase signaling and muscle adaptation response in the absence of calpain 3. *Hum. Mol. Genet.* **21**, 3193–3204.
- Jaka, O., Kramerova, I., Azpitarte, M., Lopez de Munain, A., Spencer, M. & Saenz, A. (2012). C3KO mouse expression analysis: downregulation of the muscular dystrophy Ky protein and alterations in muscle aging. *Neurogenetics*, **13**, 347–357.
- Ojima, K., Kawabata, Y., Nakao, H., Nakao, K., Doi, N., Kitamura, F. *et al.* (2010). Dynamic distribution of muscle-specific calpain in mice has a key role in physical-stress adaptation and is impaired in muscular dystrophy. *J. Clin. Invest.* **120**, 2672–2683.
- Ojima, K., Ono, Y., Ottenheijm, C., Hata, S., Suzuki, H., Granzier, H. & Sorimachi, H. (2011). Non-proteolytic functions of calpain-3 in sarcoplasmic reticulum in skeletal muscles. *J. Mol. Biol.* **407**, 439–449.
- Tagawa, K., Taya, C., Hayashi, Y., Nakagawa, M., Ono, Y., Fukuda, R. *et al.* (2000). Myopathy phenotype of transgenic mice expressing active site-mutated inactive p94 skeletal muscle-specific calpain, the gene product responsible for limb girdle muscular dystrophy type 2A. *Hum. Mol. Genet.* **9**, 1393–1402.
- Sorimachi, H., Toyama-Sorimachi, N., Saido, T. C., Kawasaki, H., Sugita, H., Miyasaka, M. *et al.* (1993). Muscle-specific calpain, p94, is degraded by autolysis immediately after translation, resulting in disappearance from muscle. *J. Biol. Chem.* **268**, 10593–10605.
- Sorimachi, H., Kinbara, K., Kimura, S., Takahashi, M., Ishiura, S., Sasagawa, N. *et al.* (1995). Muscle-specific calpain, p94, responsible for limb girdle muscular dystrophy type 2A, associates with connectin through IS2, a p94-specific sequence. *J. Biol. Chem.* **270**, 31158–31162.

23. Kinbara, K., Sorimachi, H., Ishiura, S. & Suzuki, K. (1997). Muscle-specific calpain, p94, interacts with the extreme C-terminal region of connectin, a unique region flanked by two immunoglobulin C2 motifs. *Arch. Biochem. Biophys.* **342**, 99–107.
24. Kinbara, K., Ishiura, S., Tomioka, S., Sorimachi, H., Jeong, S. Y., Amano, S. *et al.* (1998). Purification of native p94, a muscle-specific calpain, and characterization of its autolysis. *Biochem. J.* **335**, 589–596.
25. Ono, Y., Torii, F., Ojima, K., Doi, N., Yoshioka, K., Kawabata, Y. *et al.* (2006). Suppressed disassembly of autolyzing p94/CAPN3 by N2A connectin/titin in a genetic reporter system. *J. Biol. Chem.* **281**, 18519–18531.
26. Hayashi, C., Ono, Y., Doi, N., Kitamura, F., Tagami, M., Mineki, R. *et al.* (2008). Multiple molecular interactions implicate the connectin/titin N2A region as a modulating scaffold for p94/calpain 3 activity in skeletal muscle. *J. Biol. Chem.* **283**, 14801–14814.
27. Ojima, K., Ono, Y., Doi, N., Yoshioka, K., Kawabata, Y., Labeit, S. & Sorimachi, H. (2007). Myogenic stage, sarcomere length, and protease activity modulate localization of muscle-specific calpain. *J. Biol. Chem.* **282**, 14493–14504.
28. Natsume, T., Yamauchi, Y., Nakayama, H., Shinkawa, T., Yanagida, M., Takahashi, N. & Isobe, T. (2002). A direct nanoflow liquid chromatography-tandem mass spectrometry system for interaction proteomics. *Anal. Chem.* **74**, 4725–4733.
29. Sun, H. & Hunter, T. (2012). Poly-small ubiquitin-like modifier (PolySUMO)-binding proteins identified through a string search. *J. Biol. Chem.* **287**, 42071–42083.
30. Corda, D., Colanzi, A. & Luini, A. (2006). The multiple activities of CtBP/BARS proteins: the Golgi view. *Trends Cell Biol.* **16**, 167–173.
31. Chinnadurai, G. (2009). The transcriptional corepressor CtBP: a foe of multiple tumor suppressors. *Cancer Res.* **69**, 731–734.
32. Ono, Y., Ojima, K., Torii, F., Takaya, E., Doi, N., Nakagawa, K. *et al.* (2010). Skeletal muscle-specific calpain is an intracellular Na⁺-dependent protease. *J. Biol. Chem.* **285**, 22986–22998.
33. Matsuoka, S., Ballif, B. A., Smogorzewska, A., McDonald, E. R., 3rd, Hurov, K. E., Luo, J. *et al.* (2007). ATM and ATR substrate analysis reveals extensive protein networks responsive to DNA damage. *Science*, **316**, 1160–1166.
34. Kuppaswamy, M., Vijayalingam, S., Zhao, L. J., Zhou, Y., Subramanian, T., Ryerse, J. & Chinnadurai, G. (2008). Role of the PLDLS-binding cleft region of CtBP1 in recruitment of core and auxiliary components of the corepressor complex. *Mol. Cell. Biol.* **28**, 269–281.
35. Herasse, M., Ono, Y., Fougerousse, F., Kimura, E., Stockholm, D., Beley, C. *et al.* (1999). Expression and functional characteristics of calpain 3 isoforms generated through tissue-specific transcriptional and posttranscriptional events. *Mol. Cell. Biol.* **19**, 4047–4055.
36. duVerle, D. A., Ono, Y., Sorimachi, H. & Mamitsuka, H. (2011). Calpain cleavage prediction using multiple kernel learning. *PLoS One*, **6**, e19035.
37. Ma, H., Shih, M., Fukiage, C., Azuma, M., Duncan, M. K., Reed, N. A. *et al.* (2000). Influence of specific regions in Lp82 calpain on protein stability, activity, and localization within lens. *Invest. Ophthalmol. Visual Sci.* **41**, 4232–4239.
38. Bakay, M., Wang, Z., Melcon, G., Schiltz, L., Xuan, J., Zhao, P. *et al.* (2006). Nuclear envelope dystrophies show a transcriptional fingerprint suggesting disruption of Rb-MyoD pathways in muscle regeneration. *Brain*, **129**, 996–1013.
39. Mikkelsen, T. S., Wakefield, M. J., Aken, B., Amemiya, C. T., Chang, J. L., Duke, S. *et al.* (2007). Genome of the marsupial *Monodelphis domestica* reveals innovation in non-coding sequences. *Nature*, **447**, 167–177.
40. Jurka, J., Kapitonov, V. V., Kohany, O. & Jurka, M. V. (2007). Repetitive sequences in complex genomes: structure and evolution. *Annu. Rev. Genomics Hum. Genet.* **8**, 241–259.
41. Riefler, G. M. & Firestein, B. L. (2001). Binding of neuronal nitric-oxide synthase (nNOS) to carboxyl-terminal-binding protein (CtBP) changes the localization of CtBP from the nucleus to the cytosol: a novel function for targeting by the PDZ domain of nNOS. *J. Biol. Chem.* **276**, 48262–48268.
42. Lin, X., Sun, B., Liang, M., Liang, Y. Y., Gast, A., Hildebrand, J. *et al.* (2003). Opposed regulation of corepressor CtBP by SUMOylation and PDZ binding. *Mol. Cell*, **11**, 1389–1396.
43. Dammer, E. B. & Sewer, M. B. (2008). Phosphorylation of CtBP1 by cAMP-dependent protein kinase modulates induction of CYP17 by stimulating partnering of CtBP1 and 2. *J. Biol. Chem.* **283**, 6925–6934.
44. Kitamura, N., Motoi, Y., Mori, A., Tatsumi, H., Nemoto, S., Miyoshi, H. *et al.* (2009). Suppressive role of C-terminal binding protein 1 in IL-4 synthesis in human T cells. *Biochem. Biophys. Res. Commun.* **382**, 326–330.
45. Bhambhani, C., Chang, J. L., Akey, D. L. & Cadigan, K. M. (2011). The oligomeric state of CtBP determines its role as a transcriptional co-activator and co-repressor of Wingless targets. *EMBO J.* **30**, 2031–2043.
46. Kajimura, S., Seale, P., Tomaru, T., Erdjument-Bromage, H., Cooper, M. P., Ruas, J. L. *et al.* (2008). Regulation of the brown and white fat gene programs through a PRDM16/CtBP transcriptional complex. *Genes Dev.* **22**, 1397–1409.
47. Perissi, V., Scafoglio, C., Zhang, J., Ohgi, K. A., Rose, D. W., Glass, C. K. & Rosenfeld, M. G. (2008). TBL1 and TBLR1 phosphorylation on regulated gene promoters overcomes dual CtBP and NCoR/SMRT transcriptional repression checkpoints. *Mol. Cell*, **29**, 755–766.
48. Purbey, P. K., Singh, S., Notani, D., Kumar, P. P., Limaye, A. S. & Galande, S. (2009). Acetylation-dependent interaction of SATB1 and CtBP1 mediates transcriptional repression by SATB1. *Mol. Cell. Biol.* **29**, 1321–1337.
49. Stern, M. D., Aihara, H., Roccaro, G. A., Cheung, L., Zhang, H., Negeri, D. & Nibu, Y. (2009). CtBP is required for proper development of peripheral nervous system in *Drosophila*. *Mech. Dev.* **126**, 68–79.
50. Wang, S. Y., Iordanov, M. & Zhang, Q. (2006). c-Jun NH2-terminal kinase promotes apoptosis by down-regulating the transcriptional co-repressor CtBP. *J. Biol. Chem.* **281**, 34810–34815.
51. Phelps, R. A., Chidester, S., Dehghanizadeh, S., Phelps, J., Sandoval, I. T., Rai, K. *et al.* (2009). A

- two-step model for colon adenoma initiation and progression caused by APC loss. *Cell*, **137**, 623–634.
52. Tompa, P. (2012). Intrinsically disordered proteins: a 10-year recap. *Trends Biochem. Sci.* **37**, 509–516.
 53. Moldoveanu, T., Gehring, K. & Green, D. R. (2008). Concerted multi-pronged attack by calpastatin to occlude the catalytic cleft of heterodimeric calpains. *Nature*, **456**, 404–408.
 54. Hanna, R. A., Campbell, R. L. & Davies, P. L. (2008). Calcium-bound structure of calpain and its mechanism of inhibition by calpastatin. *Nature*, **456**, 409–412.
 55. Sato, N., Kawahara, H., Toh-e, A. & Maeda, T. (2003). Phosphorelay-regulated degradation of the yeast Ssk1p response regulator by the ubiquitin-proteasome system. *Mol. Cell. Biol.* **23**, 6662–6671.
 56. Ono, Y., Shimada, H., Sorimachi, H., Richard, I., Saido, T. C., Beckmann, J. S. *et al.* (1998). Functional defects of a muscle-specific calpain, p94, caused by mutations associated with limb-girdle muscular dystrophy type 2A. *J. Biol. Chem.* **273**, 17073–17078.
 57. Almenar-Queralt, A., Gregorio, C. C. & Fowler, V. M. (1999). Tropomodulin assembles early in myofibrillogenesis in chick skeletal muscle: evidence that thin filaments rearrange to form striated myofibrils. *J. Cell Sci.* **112**, 1111–1123.
 58. Pappas, C. T., Bhattacharya, N., Cooper, J. A. & Gregorio, C. C. (2008). Nebulin interacts with CapZ and regulates thin filament architecture within the Z-disc. *Mol. Biol. Cell*, **19**, 1837–1847.
 59. Katoh, K., Asimenos, G. & Toh, H. (2009). Multiple alignment of DNA sequences with MAFFT. *Methods Mol. Biol.* **537**, 39–64.
 60. Heger, A. & Holm, L. (2000). Rapid automatic detection and alignment of repeats in protein sequences. *Proteins*, **41**, 224–237.
 61. duVerle, D., Takigawa, I., Ono, Y., Sorimachi, H. & Mamitsuka, H. (2010). CaMPDB: a resource for calpain and modulatory proteolysis. *Genome Inform.* **22**, 202–213.